Title:
L_0-Regularization based Material Design for Hexahedral Mesh Models

Authors:
Haoxiang Li, haoxiang002@e.ntu.edu.sg, Nanyang Technological University, Singapore
Jianmin Zheng, asjmzheng@ntu.edu.sg, Nanyang Technological University, Singapore

Keywords:
Material Design, FEM, Hexahedral mesh, L_0 Regularization, Nonlinear Optimization

DOI: 10.14733/cadconfP.2021.314-318

Introduction:

The deformation behavior of an elastic object depends on its underlying material. We propose to design material distribution of an elastic object by specifying forces applied to some positions of the object and the respective desired deformation. The design problem is then converted into optimizing the material assignment for individual elements of the object to match the specified deformation behavior. Xu et al. [14] presented an interactive approach to solve the problem for tetrahedral meshes. Our work is focused on hexahedral meshes, which have some advantages in finite element analysis and engineering applications [3]. We consider first-order hexahedral elements. While the fully automated generation of hexahedral meshes is challenging [2, 17, 7, 4], the accuracy and simulation speed of the first-order hexahedrons are much better than tetrahedrons [8, 11, 9]. Hence the hexahedral meshes are a popular representation in numerical homogenization [6], microstructure design [10, 18], and topology optimization [12, 13].

We also propose to use L_0-regularization based optimization for material design, which is especially suitable for objects with sparsely distributed materials. Previous works usually use L_2-regularization in their optimization, which makes the parameters of the material be smoothly distributed. However, sparsely distributed materials are often seen in real applications, which also facilitate 3D printing. Note that L_0-regularization is known to encourage sparsity [15, 16]. In this work, we demonstrate that the L_0-regularization is suitable for material design of hexahedral meshes with sparse material distribution. Overall, the contributions of the paper are in two aspects:

- We propose a new material design method for hexahedral mesh models, which is suitable for fast simulation and also achieves good accuracy.
- We formulate the problem as a minimization problem with L_0 regularization to encourage sparse distribution of material.

Main Idea and Method:

The input to our problem is a hexahedral mesh with specified forces $f \in R^{3b}$ and displacements $\bar{u} \in R^{3c}$ on some selected vertices. We need to find a heterogeneous Young's modulus' distribution $E \in R^m$ such that the displacement of selected vertices of the mesh will conform to what user-specified before when the mesh is applied with prescribed forces. Our basic idea is to use L_0 regularization for the material design problem of hexahedral meshes. It is observed that many objects in real life have the clustering of similar materials in one section, which conforms to the idea of L_0 regularization. Compared with L_2

regularization, L_0 regularization prompts more sparse distribution. Therefore, we formulate our method using L_0 regularization. The main steps of our method can be stated as follows:

- Build finite element equations for hexahedral elements.
- Construct the objective function that measures the difference between user-specified displacements and displacements.
- Solve the L_0 regularization based minimization problem numerically.

(1) Construction of Finite Element Equations

Now we briefly describe the finite element equations of hexahedral elements. We limit our discussion to first-order, linear isotropic hexahedral elements. In each hexahedron, the element stiffness matrix k_e [5] that relates forces and displacements is:

$$k_e = \iiint_{\Omega^{(e)}} B^T D B \mathrm{d}\Omega^{(e)} = \int_{-1}^{1}\int_{-1}^{1}\int_{-1}^{1} \mathbf{B}^{\mathrm{T}}\mathbf{D}\mathbf{B}|\mathbf{J}|\mathrm{d}\xi\mathrm{d}\eta\mathrm{d}\zeta \approx \sum_{i=1}^{NG}\sum_{j=1}^{NG}\sum_{k=1}^{NG} \omega_i\omega_j\omega_k \mathbf{B}^{\mathrm{T}}\mathbf{D}\mathbf{B}|\mathbf{J}| \tag{2.1}$$

Here, element domain $\Omega^{(e)}$ is defined in physical coordinate. Matrix D is the elasticity matrix to relate stress and strain. Matrix B is the strain-displacement matrix that needs to be computed from shape functions. Shape functions are used to determine the value of the state variable at any point of the element based on values of the state variable on different nodes of that element. To deal with different shape functions for different hexahedron elements, we map different hexahedron elements to reference elements with the same shape functions. ξ, η, and ζ represent the reference coordinate. Jacobian matrix J is used to map the derivatives of shape functions from physical to reference coordinate. Since the above integration process is difficult to solve, we use Gauss integration. Before optimization, we also specify sufficient fix points to remove the rigid degrees of freedom, which make the global stiffness matrix become non-singular.

(2) Construction of the Objective Function.

Since different mesh displacements U are uniquely determined by underlying material distribution through solving a linear system $K(E)U = F$, we are able to design a material distribution $E \in R^m$ to match user-specified displacements $\bar{u}$. we can recast the material design problem as a minimization problem:

$$\min_{E} \|A_c U - \bar{u}\|^2 + R(E) \quad \text{s.t. } E \in [E_{\min}, E_{\max}] \tag{2.2}$$

where $A_c \in R^{3c\times 3n}$ is a selection matrix to map full displacements to the displacements on selected vertices c. $U \in R^{3n}$ is the displacement vector of all vertices. $\bar{u} \in R^{3c}$ is the displacement vector of selected vertices specified by users. $R(E)$ is a regularization term to enforce our prior on the distribution of material parameters. $E_{\min} \in R^m$ and $E_{\max} \in R^m$ are box constraints set by the user, e.g. we can enforce non-negative Young's modulus by setting $E_{\min} = \mathbf{0}$ and $E_{\max} = +\infty$.

Throughout the paper, we use the relative handle displacement error ε_u to evaluate our optimization result. The ε_u is defined as:

$$\varepsilon_u = \frac{||A_c U - \bar{u}||}{||\bar{u}||} \tag{2.3}$$

where ε_u can be formulated as a percentage to evaluate the optimized results.

(3) L_0-Optimization

Let $D(E) = \|A_c U - u\|^2$ and then we focus on the regularization term $R(E)$. If Young's modulus E is

optimized by L_0-regularization, the objective function becomes:

$$\min_E D(E) + \lambda \sum_{(i,j)\in N} \|E_i - E_j\|_0 \tag{2.4}$$

Note that the objective function of the minimization problem is not differentiable. To efficiently solve the problem, we introduce the auxiliary variable $P_{i,j} = E_i - E_j$. Then our problem becomes

$$\min_E D(E) + \lambda \sum_{(i,j)\epsilon N} \|P_{i,j}\|_0 \text{ s.t. } P_{i,j} = E_i - E_j \tag{2.5}$$

Since $P_{i,j} = E_i - E_j$ is the equality constraint, we can use the alternating direction method of multipliers (ADMM) to solve the problem. We then formulate the augmented Lagrangian as:

$$D(E) + \sum_{(i,j)\in N} \left(\lambda \|P_{i,j}\|_0 + \frac{r_p}{2} \|E_i - E_j - P_{i,j}\|^2 + \lambda_{ij} (E_i - E_j - P_{i,j})\right) \tag{2.6}$$

Here, the constant value doesn't affect optimization. we can combine the last two terms as:

$$D(E) + \sum_{(i,j)\in N} \left(\lambda||P_{i,j}||_0 + \frac{r_p}{2}||E_i - E_j - P_{i,j} + \frac{\lambda_{ij}}{r_p}||^2\right) \tag{2.7}$$

Then, the problem can be solved by the iterative method:

1. Firstly, we fix E and optimize the auxiliary variable P.

$$\min_P \sum_{(i,j)\in N} \left(\lambda||P_{i,j}||_0 + \frac{r_p}{2}||E_i - E_j - P_{i,j} + \frac{\lambda_{ij}}{r_p}||^2\right) \tag{2.8}$$

   This problem becomes a hard threshold problem. The auxiliary variable P can be optimized pointwisely by setting $P_{i,j}$ equals to zero or not.
2. Secondly, we fix the auxiliary variable P and optimize E. The L_0 term is no longer active in this step. Therefore, we have:

$$\min_E D(E) + \sum_{(i,j)\in N} \frac{r_p}{2}||E_i - E_j - P_{i,j} + \frac{\lambda_{ij}}{r_p}||^2 \tag{2.9}$$

   Notice that the current objective function is derivable. We can directly solve this problem by either nonlinear conjugate gradient or LBFGS method with box constraints.
3. In the last step, we update Lagrange Multiplier λ_{ij} the same way as the original ADMM algorithm.

Here we design the update sequence to reduce the effect of the deviation phenomenon. If we first optimize Young's modulus, the augmented term and Lagrange term also plays an important role in affecting material distribution in the first iteration. Even if we use a warm start from L_2 regularization method, these two terms may still be prone to derive away from the warm start. As a result, if this phenomenon deviates the warm start to a position that too far away from optimal, it'll cause difficulty in converging to a high-precision solution.

Examples:

To demonstrate the capability of our algorithm, we have applied the method to different models. Fig.1 and Fig.2 compare the optimized result between L_2 and L_0 regularization. Fig.3 is a showcase of the

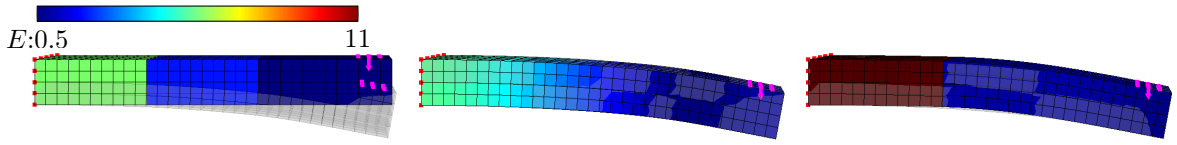

(a) Input Configuration (b) L_2 regularization, $\varepsilon_u = 0.29\%$ (c) L_0 regularization, $\varepsilon_u = 0.84\%$

Fig. 1: Comparison between L_2 regularization and our L_0 regularization on bar model. (a) Input configuration, including fix points, user-specified forces, and the target displacements computed from ground truth material distribution; (b) Optimized result of L_2 regularization; (c) Optimized result of our L_0 regularization.

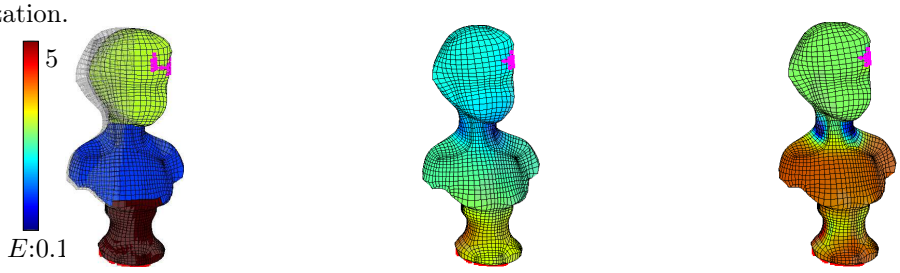

(a) Input Configuration (b) L_2 regularization, $\varepsilon_u = 2.61\%$ (c) L_0 regularization, $\varepsilon_u = 2.27\%$

Fig. 2: Comparison between L_2 and L_0 regularization on human sculpture model. (a) Input configuration of the human sculpture model; (b) Optimized result of L_2 regularization; (c) Optimized result of our L_0 regularization.

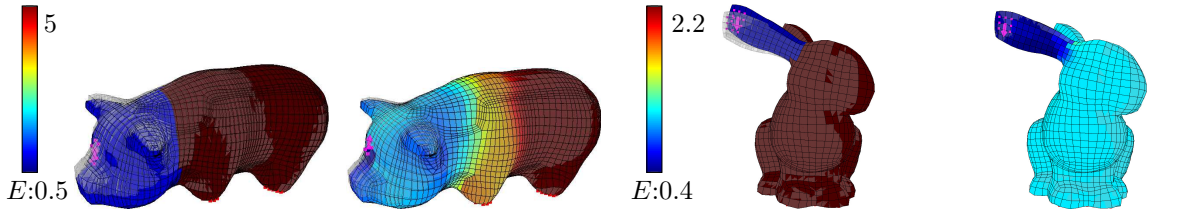

(a) Input Configuration (b) L_0 regularization (c) Input Configuration (d) L_0 regularization

Fig. 3: L_0 regularization effect on pig and bunny model. (a) Input configuration of the pig model; (b) Corresponding L_0 regularization result, $\varepsilon_u = 1.63\%$; (c) Input configuration of the bunny model; (d) Corresponding L_0 regularization result, $\varepsilon_u = 1.31\%$

L_0 regularization effect on different models. In our experiments, we supposed ground truth material distributions. The displacements of the selected vertices can be computed from ground truth material distributions. Then, we can use the computed displacements as input to our algorithm.

Conclusions:

This paper has presented an efficient numerical method for optimizing Young's modulus distribution over a hexahedral mesh to achieve the desired deformation. The method allows imposing box constraints easily. The use of L_0 regularization in the optimization shows some advantages especially for sparsely distributed materials. In future, we will compare our method with other discrete methods like material dithering [14] and decision tree [1].

References:

[1] Bickel, B., Bächer, M., Otaduy, M. A., Lee, H. R., Pfister, H., Gross, M., and Matusik, W. Design and fabrication of materials with desired deformation behavior. ACM Transactions on Graphics (TOG)

29, 4 (2010), 1–10.
[2] Blacker, T. D., and Meyers, R. J. Seams and wedges in plastering: a 3-d hexahedral mesh generation algorithm. Engineering with computers 9, 2 (1993), 83–93.
[3] Cifuentes, A., and Kalbag, A. A performance study of tetrahedral and hexahedral elements in 3-d finite element structural analysis. Finite Elements in Analysis and Design 12, 3-4 (1992), 313–318.
[4] de Oliveira Miranda, A. C., and Martha, L. F. Hierarchical template-based hexahedral mesh generation. Engineering with Computers 34, 3 (2018), 465–474.
[5] Kim, N.-H. Introduction to nonlinear finite element analysis. Springer Science & Business Media, 2014.
[6] Nesme, M., Payan, Y., and Faure, F. Animating shapes at arbitrary resolution with non-uniform stiffness. In VRIPHYS (2006).
[7] Owen, S. J., Brown, J. A., Ernst, C. D., Lim, H., and Long, K. N. Hexahedral mesh generation for computational materials modeling. Procedia engineering 203 (2017), 167–179.
[8] Ramos, A., and Simoes, J. Tetrahedral versus hexahedral finite elements in numerical modelling of the proximal femur. Medical engineering & physics 28, 9 (2006), 916–924.
[9] Schneider, T., Hu, Y., Gao, X., Dumas, J., Zorin, D., and Panozzo, D. A large scale comparison of tetrahedral and hexahedral elements for finite element analysis. arXiv preprint arXiv:1903.09332 (2019).
[10] Schumacher, C., Bickel, B., Rys, J., Marschner, S., Daraio, C., and Gross, M. Microstructures to control elasticity in 3d printing. ACM Transactions on Graphics (TOG) 34, 4 (2015), 1–13.
[11] Tadepalli, S. C., Erdemir, A., and Cavanagh, P. R. Comparison of hexahedral and tetrahedral elements in finite element analysis of the foot and footwear. Journal of biomechanics 44, 12 (2011), 2337–2343.
[12] Wu, J., Aage, N., Westermann, R., and Sigmund, O. Infill optimization for additive manufacturing-approaching bone-like porous structures. IEEE transactions on visualization and computer graphics 24, 2 (2017), 1127–1140.
[13] Wu, Z., Xia, L., Wang, S., and Shi, T. Topology optimization of hierarchical lattice structures with substructuring. Computer Methods in Applied Mechanics and Engineering 345 (2019), 602–617.
[14] Xu, H., Li, Y., Chen, Y., and Barbič, J. Interactive material design using model reduction. ACM Transactions on Graphics (TOG) 34, 2 (2015), 1–14.
[15] Xu, L., Lu, C., Xu, Y., and Jia, J. Image smoothing via l 0 gradient minimization. In Proceedings of the 2011 SIGGRAPH Asia Conference (2011), pp. 1–12.
[16] Zhang, J., Zhao, D., and Gao, W. Group-based sparse representation for image restoration. IEEE Transactions on Image Processing 23, 8 (2014), 3336–3351.
[17] Zhang, Y., Hughes, T. J., and Bajaj, C. L. An automatic 3d mesh generation method for domains with multiple materials. Computer methods in applied mechanics and engineering 199, 5-8 (2010), 405–415.
[18] Zhu, B., Skouras, M., Chen, D., and Matusik, W. Two-scale topology optimization with microstructures. ACM Transactions on Graphics (TOG) 36, 4 (2017), 1.